Three and Four Dimensional Geometric Analyses of Causal Regions During Inflation

Cole Meldorf

May 28, 2022

A Thesis Presented for the Degree of Bachelor of Science

Department of Astrophysics

University of Chicago

Abstract

This thesis expands upon the work done in Hogan & Meyer (2022) concerning the theory that the symmetries underlying quantum entanglement of inflationary horizons may explain certain suggestive regions of the correlation function of the Cosmic Microwave Background (CMB) temperature anisotropies. We seek to create higher dimensional, interactive versions of figures explaining this theory as a pedagogical tool for the understanding of this complicated subject. Using an accompanying python notebook to this paper, we explain some important predictions of this theory using our higher dimensional figures. In particular, we replicate the geometric arrangement of intersecting spherical horizons from Hogan & Meyer (2022) as well as adding the null geodesics of photons traversing them. We explore this system in three and four dimensions in order to demonstrate results such as that in the $\pi < \theta < 3\pi/4$ region $\mathrm{C}(\theta) = 0$. In the appendix, we derive the null geodesics in an exponentially inflating spacetime used in the creation of these figures. These predicted values of the CMB correlation function using this theory seem to agree more strongly with the real world data than standard inflation theories; as such this thesis hopes to make this theory more accessible for further study.

1 Introduction

The theory of inflation is currently our best model of the primordial universe. This theory postulates that all of modern large scale structure originates from quantum fluctuations expanded to gigantic sizes by the expansion of space.[1] In addition, these curvature fluctuations are imprinted onto the CMB, allowing us to measure the cosmological structure of the universe only a few hundred thousand years after the big bang. [2]

However, our models for the patterns in these CMB fluctuations have several discrepancies with the actual measurements, see Figure 1. This has lead to questions about the validity of the current theory of inflation or propositions of potential extensions to it.

[4] One particularly suggestive result comes from analysis of the angular correlation function:

$$C(\theta) = \langle \Delta_a \Delta_b \rangle_{\angle ab=\theta} \tag{1}$$

In essence, this represents the whole sky average value of deviation from the mean CMB temperature of the over every pair of points a and b separated by an angle θ. Evaluating this function for real CMB data returns an interesting result:

$$C(90^\circ) \simeq 0 \tag{2}$$

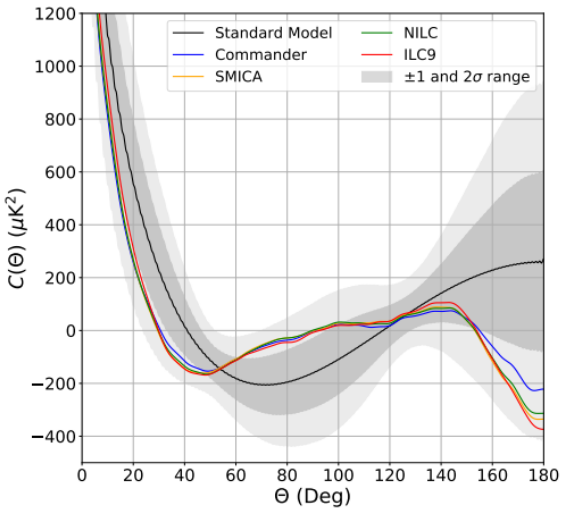

Figure 1: Above, the angular correlation function C(θ) of the CMB temperature anisostropy is plotted against θ, measured with the WMAP and Planck satellites. Different colors show results for different foreground galactic data subtraction algorithms: ILC9 from WMAP, and NILC, Commander, and SMICA from Planck. The measured angular correlation functions are plotted alongside the expected values (with 1σ and 2σ uncertainties) from standard inflationary models, shown by the shaded bands. [3].

A vanishing value at such an important angle strongly hints some sort of intrinsic symmetry. [5] In addition, there is a surprising dip into negative values for the angular correlation function (anticorrelation) for angles greater than 135°. These facts are typically considered to be statistical coincidences of our particular universe, as the standard model of inflation does not make a singular prediction for the angular correlation function but rather gives a collection of different possibilities with different statistical properties. [3] Examples of this variation are shown in Figure 2 However, recent papers such as [3] suggest that these correlations could actually reflect the nature of quantum gravity. In particular, through analysis of the geometry of spacetime during inflation, one can study the nonlocal causal coherence of quantum gravity. This thesis attempts to extend their work by visualizing the geometry that causes these particular angular correlations so as to assist further study of the nature of quantum gravity through a cosmological lens.

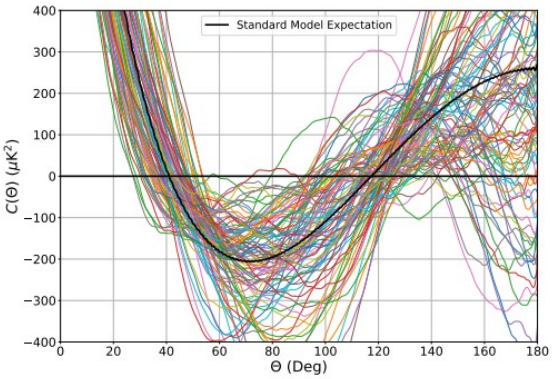

Figure 2: Above we show one hundred random predictions of the standard model of inflation. This range of expectations has allowed physicists to claim that certain features of the CMB correlation function are statistical flukes of our universe. But holographic theories could possibly provide theoretical explanations for these features. [3]

2 Methods

It is not the purpose of this thesis to fully derive a holographic theory of quantum gravity, but to rather expand upon and clarify previous work. The spacetime diagrams common in many papers on this subject are 2d representations of what is fundamentally a 4d phenomenon. Though we cannot realistically expect to accurately portray four dimensions in a two dimensional medium, 3d projections combined with a "sliding" fourth dimension can create a much more understandable representation of the systems explored. In order to do so, this paper is accompanied by a python notebook where interactive figures are included. This work makes extensive use of the "interact" library from ipywidgets. The python notebook is available here: `https://colab.research.google.com/drive/1AdjjcpwqbTvqR9GzVd7UmdUQQoLhLFWw?usp=sharing`.

3 Building a Visual Model

First, consider the horizon of an observer at the end of inflation. Frozen in time, this can be visualized as a 3-sphere centered on the observer. Consider one part of this horizon. A circle subtended by some angle θ is the set of

points averaged over for the angular correlation function for this specific location on the horizon, see Figure 3.

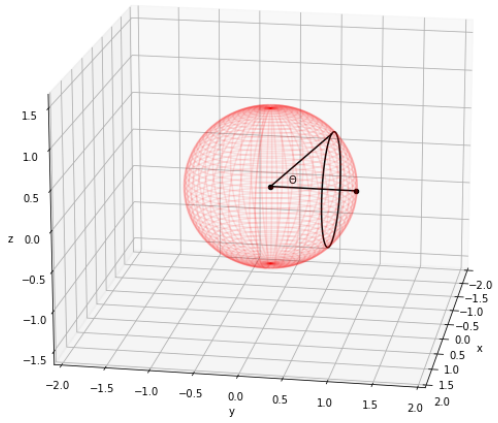

Figure 3: A visualization of the region considered when evaluating the CMB two-point correlation function. If the central dot is our observer, the black circle on the observer's horizon represents the points at an angle θ which we average over to determine C(θ). The distance from the center of A to this circle is defined as d_A, and is given by cos(θ).

To evaluate the correlation function, $C(\theta)$, this average is then performed for every point on the horizon. A useful quantity for later analysis will be the separation from the center of A to the circle defined by θ. We call this value d_A and evaluate it as simply cos(θ).

Now we would like to consider what information is able to reach our observer. Since information travels at the speed of light, we can visualize the region information can reach with a 3-sphere, which is really a 3 dimensional slice of a 4d light cone. Hence, any sphere with radius $c\Delta t$ that encloses our observer can be considered causally connected to them. If we consider a 3-sphere that just intersects our observer, which we will call sphere B, we can recover a geometry shown in Figure 4. When constructed in this way the B sphere bounds the flow of information to and from the center of A. [3]

While only one example is shown here, there is a B sphere for every point on the horizon. Note that, while we included the circle subtended by

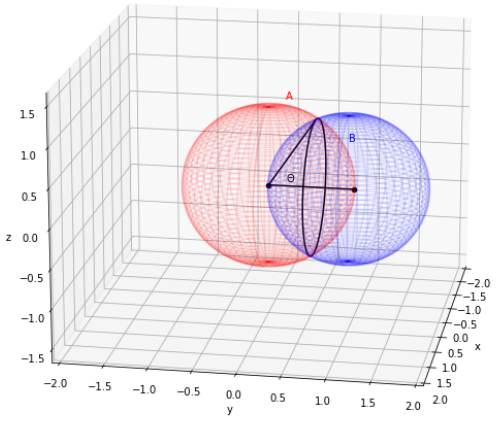

Figure 4: Building on Figure 3, we now include the "B" sphere, which intersects the A sphere at its center and at a circle on the surface of A defined by an angle θ. The B sphere bounds the flow of information to and from the center of A. [3]

angle θ as a demonstration of the correlation function, this circle is also the intersection between our observers horizon and the B sphere. In fact, there is a B sphere defined for every value of θ. However, sweeping through values of θ changes the radius and position of the B sphere, as can be demonstrated in the attached interactive figures in cell 2 and 3. (Explanations of the sliders are included as comments above the interactive figures.) Mathematically speaking, assuming the original horizon sphere (red in the figures) has a radius of 1, then the B sphere will have a radius:

$$R_B = \frac{1}{2\cos(\theta)}. \tag{3}$$

Assuming we keep the observer's horizon fixed at the origin, the center of the B sphere will be located at a distance

$$d_B = \cos(\theta) - \frac{\cos(2\theta)}{2\cos(\theta)} \tag{4}$$

from the center of the observer's horizon. These expressions are derived from the constraints that firstly, the B sphere intersects with the center

of A, as it defines the region that is causally connected with A. Secondly, we require that the B sphere intersects with A at the circle defined by the angle θ. At first, it might be confusing why all of B contributes to the correlation function, as you can easily draw photon paths from B to the center of A without intersecting the circle where C(θ) is calculated. However, the principle of holographic universality that this theory is built upon implies that the mean contribution to C(θ) on the surface of a sphere is the same as the the contribution at the center of the sphere. [3] Therefore we can calculate the B sphere's contribution to C(θ) as long as we can calculate it at B's center.

For a given value of θ we wish to consider information propagating in from one direction, which we take to be the y axis where $\theta = 0$. In this way, one can think of the information that we are considering as a large moving plane, or the horizon of sphere that is infinitely large. [3]

In addition, we can construct another sphere which acts as a causal boundary for information on the surface of the A sphere. We call this the C sphere. The C sphere has a comoving radius of:

$$R_C = 2\sin(\theta_A/2) \tag{5}$$

and is centered at y = R_A, which we have taken to be 1. When constructed in this way the C sphere bounds the flow of information to and from the surface of A. [3] Spheres A, B, and C are shown in Figure 5. Note how all 3 spheres intersect at a common circle defined by an angle θ from the y axis, as desired. The relationships between the sizes and offsets of the various spheres are shown in number 1 in the attached notebook, an interactive version of Figures 3 through 5.

As a culmination of the model built so far in cell 3 we have taken a 2d slice of the system and plotted the offsets (from the common circle) and radii of the various spheres as a function of θ, see Figure 6. This figure is an interactive and ideally more intuitive analog of Figures 8 and 9 in [3].

From this figure we can make an important conclusion. Recall that the correlation function is determined by information causally connected with both the common circle and the A and B centers. Thus it follows that when the distance from the center of A to B (i.e. the radius of B) is larger than the distance from A to the common circle (d_A) the angular correlation function should drop to zero. [3] Solving for where $d_A < R_B$ yields:

$$\pi < \theta < 3\pi/4 \implies C(\theta) = 0. \tag{6}$$

This is a desired result of this theory that seems to agree with measured results, which we will explore in the following section. Of course, there is

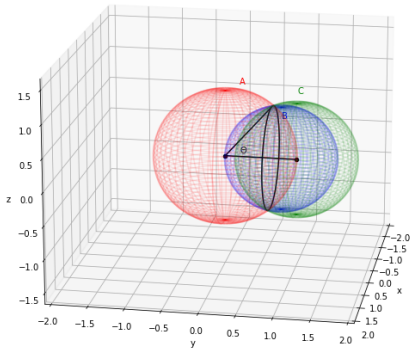

Figure 5: Building on Figure 4, we now include the "C" sphere, whose center lies on A's horizon but also intersects with A and B at the same common circle. The C sphere bounds the flow of information to points on the surface of A. [3]

also the region $\pi/4 < \theta < \pi$ where $d_A < R_B$, but since we are considering information as coming in from the $\theta = 0$ direction, any information that reaches the center of A must cross through B, and hence become correlated.

In addition, we can make theoretical predictions on the $\theta > 3\pi/4$ region. In this region $d_A > R_B$ so we expect some correlation. However, due to the fact that the B sphere is now in the antipodal region, we expect the correlation to be negative. [3]

3.1 Comparisons to the CMB Correlation Function

Constructing this system of spheres will allow us to visualize how holographic theories of quantum gravity can better predict the CMB correlation function. Real-world data for the CMB correlation function, measured with the WMAP and Planck satellites is shown in Figure 1.

A fully mature theory of quantum gravity and of inflation should be able to predict a CMB correlation function similar to this. Note that the standard model prediction, shown in black, is in 2σ disagreement in many portions of the distribution, and noticeably does not predict the $90 < \theta < 135$ region where $C(\theta) \simeq 0$. With an additional dipole correction, the $C(\theta) \simeq 0$ region in the data is even more apparent, see Figure 7.

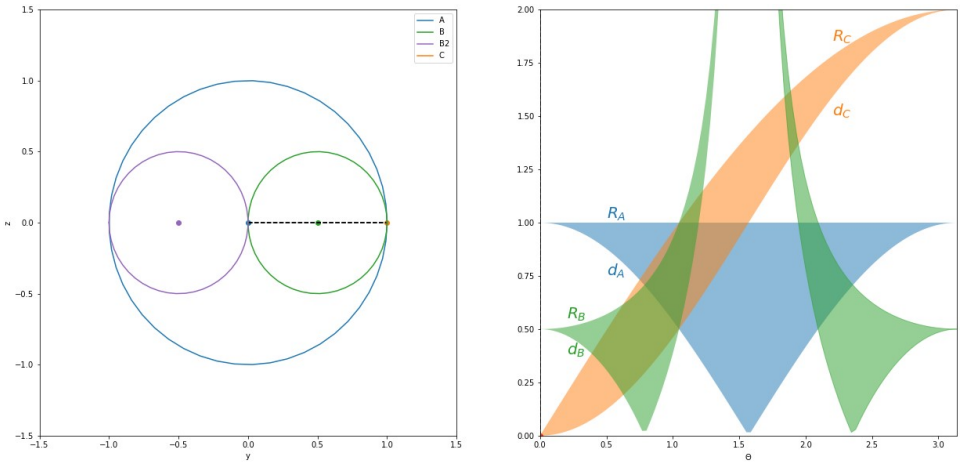

Figure 6: *Left:* A 2d slice of 5, however we have also included the B sphere of opposite parity. This figure is interactive in the attached python notebook, allowing you to slide over values of θ (the t slider) to see the changing geometries. *Right:* A plot of the radii of each sphere and their separation from the common circle as a function of θ. Note the regions where $d_A < R_B$ as these will be important shortly.

In cell 4 we provide a three dimensional visualization of the process driving the predicted CMB correlation function. In the rightmost figure, we show the theoretical CMB correlation function, where the current value of $C(\theta)$ and θ is marked with a point. By moving the slider associated with θ we can explore different regions of this function. The construction of this theoretical correlation function involves more than just the horizon arguments used in this paper thus far, including correcting for dipole fluctuations and the changing expansion rate predicted by slow-roll inflation. [6] This is beyond the scope of this work, and we instead draw attention to the regions where $\mathrm{C}(\theta) = 0$ as predicted by the arguments above. For a full derivation of this curve, see [3].

In the other two figures we show two separate realizations of the horizons relevant to this problem. In the upper left, we show light cones with the same radii as the spheres we have discussing so far, essentially rendering the vertical axis into a time axis. In addition, we plot a facsimile of the "infinitely distant B sphere" mentioned previously by plotting a very large light cone. In the bottom center we show again the relationship between the A and B spheres, hoping to highlight the relationship between the positions

of the horizon spheres and the resulting correlation function.

Plotting the predicted CMB function from the holographic theory against real world data yields good, but not perfect, agreement. We include the comparison here rather than in the interactive notebook to avoid clutter, see Figure 7.

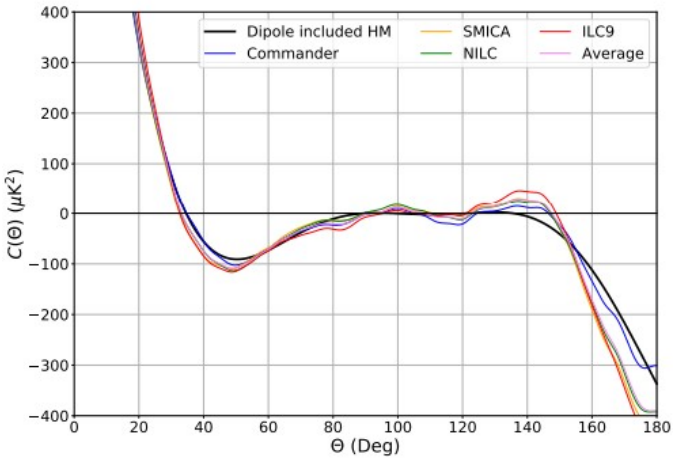

Figure 7: The Holographic model for the CMB correlation function versus the same data shown in Figure 1 with an additional dipole correction. [3] Note the $90 < \theta < 135$ region where $C(\theta) \simeq 0$ as predicted.

3.2 Photon Paths

While these geometric analyses are useful in beginning to understand the underlying symmetries governing the correlation function, the overlapping spheres can still be unintuitive even when additional dimensions are shown. Another, possibly more understandable, demonstration would be a figure which allows one to trace photon paths along their null geodesics in order to see how they are able to correlate or not correlate with our observer at the center of A. In order to do so, we need to have an analytical expression for the paths of photons in an inflationary spacetime. In the appendix (A) we derive the null geodesics for an inflating FLRW metric from basic general relativity. To build intuition for the paths photons will take, we include in cell 5 a 4d plot of photon paths in this spacetime. In the center lies an observer, and their horizon is given by the surrounding sphere. We

plot a plane of photons traveling in the negative y direction. As inflation occurs, the photons either are pushed away by the Hubble flow or are able to overcome it and reach the observer. Notice how any photon that crosses outside the horizon will proceed to infinity. You can observe this by moving the "start" slider to change the photons starting position. Once the plane of photons starts entirely outside the horizon, all of the photons are pushed away to infinity by the inflating spacetime. An example of two sets of such photon paths are shown in Figure 8.

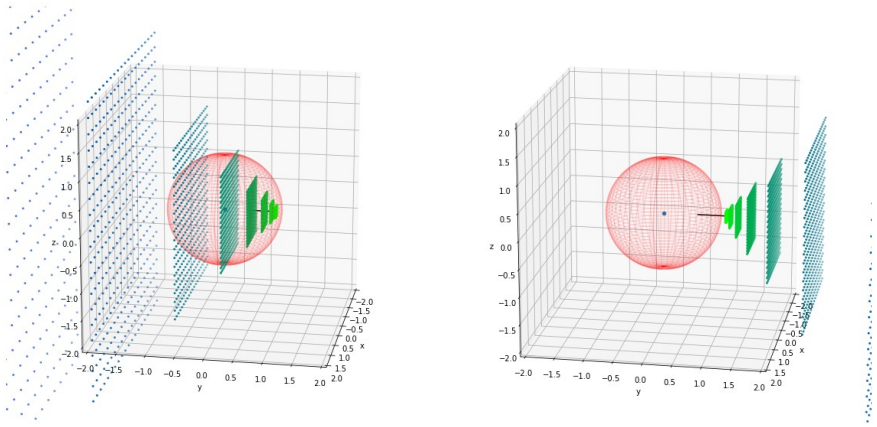

Figure 8: Two representative images of the null geodesics of photons in an inflationary spacetime. Specifically, we show ten time steps of the paths that can be scrolled over in cell 5. We color code the photons for clarity, green being earlier in time, blue being later in time. In each plot we show a 20 by 20 grid of photons moving in the negative y direction, towards an observer at the origin. We plot the horizon of the observer as a wiremesh sphere. The black line indicates the photons starting direction for clarity. *Left:* The grid of photons starts at y = 0.9, or 90% the size of the observers horizon. Note that the photon that is moving exactly radially is able to reach the observer. *Right:* The grid of photons starts at y = 1.1, or 110% the size of the observers horizon. Note no photons are able to reach the observer, even though their velocity is in the negative y direction, they are all swept away by the expansion of the universe.

With this intuition in hand we can apply these geodesics to the geometries that affect the CMB correlation function. In the final interactive figure, shown in cell 6, we plot the null geodesics of photons alongside the geometrical system we have been building up. Here we are plotting in co-moving

coordinates rather than in proper distances, so the photons appear to move in straight lines. However, a main difference between these geodesics and those in a flat, non-expanding universe is that they have a finite range in comoving coordinates, see Equation 19 in the appendix. An intuitive way to rationalize this is to recall that photons are moving at a constant velocity (c) while the universe's expansion is constantly accelerating. Thus, if allowed to go on for long enough, the universe's expansion will drastically outpace the speed of light, meaning that photons tend toward being stationary in comoving coordinates as time approaches infinity.

Plotting these geodesics alongside the geometric system we have been building up in this work allows us to directly observe the phenomena that manifest in the CMB correlation function. (This interactive figure is essentially a 4d combination of figures 10 and 11 in [3], where we show individual photons moving in time rather than light cones.) The large wiremesh spheres represent the A and B spheres discussed throughout the paper. The small blue points represent a small group of photons traveling in the inflationary spacetime in comoving coordinates. θ, the angle at which the correlation function is being affected, and time are free to be varied over with the provided sliders. Notice how in the $\pi < \theta < 3\pi/4$ region the photons are not able to reach the center of A, and are hence not able to correlate, while when $\theta > 3\pi/4$ they are able to do so. This is another visualization of the phenomenon where $\pi < \theta < 3\pi/4 \implies C(\theta) = 0$.

4 Conclusions

In this work, we have explored the symmetry-based arguments involving the causal structure of horizons that seek to explain certain regions of the CMB two point correlation function. We firstly used three dimensional interactive figures to create a more realistic and easily understandable representation of the system. In particular, using interactive figures we explore the argument that in the region $\pi < \theta < 3\pi/4 \implies C(\theta) = 0$. We resort to several different presentations of the geometric systems behind this phenomenon with the goal of creating a more universally intuitive description of the reasoning behind this symmetry. The results of [3] suggest that the 2D angular correlation function of primordial curvature may be governed by causally-coherent quantum gravity, but as we saw in Figure 7 the agreement between data and theory can still be improved. This work hopes to facilitate further investigation of this theory through our higher-dimensional analyses.

5 Acknowledgements

The author would like to thank Dr. Craig Hogan, his thesis advisor, for his infinite patience in the creation of this project. In addition he would also like to thank Dr. Stephan Meyer and Dr. Nickolay Gnedin for being final readers on this thesis, as well as Dr. Julia Brazas for running the University of Chicago Department of Astrophysics Undergraduate Thesis program.

References

[1] A. H. Guth, "Inflationary universe: A possible solution to the horizon and flatness problems," *Phys. Rev. D*, vol. 23, pp. 347–356, Jan 1981.

[2] C. L. Bennett, D. Larson, J. L. Weiland, N. Jarosik, G. Hinshaw, N. Odegard, K. M. Smith, R. S. Hill, B. Gold, M. Halpern, E. Komatsu, M. R. Nolta, L. Page, D. N. Spergel, E. Wollack, J. Dunkley, A. Kogut, M. Limon, S. S. Meyer, G. S. Tucker, and E. L. Wright, "NINE-YEAR WILKINSON MICROWAVE ANISOTROPY PROBE (WMAP) OBSERVATIONS: FINAL MAPS AND RESULTS," *The Astrophysical Journal Supplement Series*, vol. 208, p. 20, sep 2013.

[3] C. Hogan and S. S. Meyer, "Angular correlations of causally-coherent primordial quantum perturbations," *Classical and Quantum Gravity*, vol. 39, p. 055004, feb 2022.

[4] A. de Oliveira-Costa, M. Tegmark, M. Zaldarriaga, and A. Hamilton, "Significance of the largest scale CMB fluctuations in WMAP," *Physical Review D*, vol. 69, mar 2004.

[5] R. Hagimoto, C. Hogan, C. Lewin, and S. S. Meyer, "Symmetries of CMB temperature correlation at large angular separations," *The Astrophysical Journal*, vol. 888, p. L29, jan 2020.

[6] A. R. Liddle, P. Parsons, and J. D. Barrow, "Formalizing the slow-roll approximation in inflation," *Physical Review D*, vol. 50, pp. 7222–7232, dec 1994.

[7] J. B. Hartle, *Gravity: An Introduction to Einstein's General Relativity.* Benjamin Cummings, illustrate ed., Jan. 2003.

A Null Geodesics in an Inflationary Spacetime

When considering what photons are able to reach an observer at the end of inflation, it is useful to have an actual visualization of photon paths during inflation. These are found by solving the geodesic equation from general relativity for a metric that represents an inflationary spacetime.

A.1 The Radial Case

The metric for an expanding spacetime is given by the Friedmann–Lemaître –Robertson–Walker (FLRW) metric:

$$ds^2 = -dt^2 + a^2(t)\Big[\frac{dr^2}{1-kr^2} + r^2(d\theta^2 + \sin^2(\theta)d\phi^2\Big] \tag{7}$$

k is a parameter that controls the curvature of the universe; here we will assume $k = 0$. Since we are considering only radial motion, we can ignore the θ and ϕ terms, leaving us with:

$$ds^2 = -dt^2 + a^2(t)dr^2. \tag{8}$$

Since we are considering exponential inflation, $a(t) = e^t$. This expression ends up being simple enough that we can solve it from here without any additional general relativity. Enforcing that the geodesic be null and dividing both sides by dt^2 and dividing across yields:

$$a^{-2} = dr^2/dt^2 \tag{9}$$

or:

$$\pm\, e^{-t} = dr/dt. \tag{10}$$

This is easily solvable, leaving:

$$r(t) = \pm e^{-t} + c. \tag{11}$$

Plugging in t = 0 we can see that $c = r(0) - 1$ for the inward motion case. Hence our final solution is:

$$r(t) = e^{-t} + r_0 - 1 \tag{12}$$

in co-moving coordinates or

$$r(t) = e^t(e^{-t} + r_0 - 1) \tag{13}$$

in terms of proper distances.

A.2 The General Case

While more difficult than the simple algebra of the previous section, the general case can be solved with some elementary general relativity. In Cartesian coordinates, the 3 dimensional metric

$$g_{\alpha\beta} = \begin{bmatrix} -1 & 0 & 0 & 0 \\ 0 & e^{2t} & 0 & 0 \\ 0 & 0 & e^{2t} & 0 \\ 0 & 0 & 0 & e^{2t} \end{bmatrix} \tag{14}$$

has 3 Killing vectors, namely: ξ = (0,1,0,0), (0,0,1,0), and (0,0,0,1), as it is independent of all spatial coordinates. Now, by the definition of the killing vector: [7]

$$u \cdot \xi = \frac{dx^i}{d\lambda} e^{2t} = \text{constant}, \tag{15}$$

where u is the four velocity, the index i runs over the spatial coordinates, and λ in an affine parameter. Enforcing that the geodesic again be null, and exploiting equation 15 we can write

$$0 = -dt^2/d\lambda^2 + C^2 e^{-2t} \tag{16}$$

where C is some constant. Thus:

$$\frac{dt}{d\lambda} = Ce^{-t}, \tag{17}$$

and by the chain rule:

$$\frac{dx}{dt} = \frac{dx}{d\lambda}\frac{d\lambda}{dt} = Ce^{-t}. \tag{18}$$

We take the constant C to be the initial velocity in the x direction. Integrating gives:

$$x(t) = -v_{x0}e^{-t} + c. \tag{19}$$

Solving for x(0) demonstrates that c is the initial velocity plus the initial position. In proper distance coordinates we write this as:

$$x(t) = e^t(-v_{x0}e^{-t} + x_0 + v_{x0}). \tag{20}$$

The equations for $y(t)$ and $z(t)$ are the same, by symmetry. An additional constraint is that we require that the total velocity is the speed of light, so:

$$v_{x0}^2 + v_{y0}^2 + v_{z0}^2 = 1 \tag{21}$$